Available online at www.sciencedirect.com

ScienceDirect

Dyes and Pigments 77 (2008) 415−426

DYES and PIGMENTS

www.elsevier.com/locate/dyepig

Kinetic and equilibrium studies on the removal of cationic dyes from aqueous solution by adsorption onto a cyclodextrin polymer

Grégorio Crini*

Université de Franche-Comté, Laboratoire de Biologie Environnementale, EA 3184 USC INRA, Place Leclerc, 25030 Besançon cedex, France

Received 15 March 2007; received in revised form 7 July 2007; accepted 14 July 2007

Abstract

Batch adsorption experiments were carried out for the removal of basic dyes, namely C.I. Basic Blue 3, Basic Violet 3 and Basic Violet 10, from aqueous solutions using a cyclodextrin polymer. Studies concerning the effects of contact time and initial dye concentration are presented and discussed. Results of batch experiments showed that this adsorbent exhibited high sorption capacities toward basic dyes. Experimental data were analyzed using pseudo-second order kinetics, mass transfer, and intraparticle diffusion models. It was found that kinetics followed a pseudo-second order equation, suggesting that the rate-limiting step may be chemisorption. Equilibrium isotherm data were analyzed according to Langmuir and Freundlich equations. The characteristic parameters for each model have been determined. The Freundlich isotherm gave the best correlation for the adsorption of basic dyes on CDP material. On the basis of the Langmuir analysis, the maximum adsorption capacities were determined to be 53.2, 42.4 and 35.8 mg of dye per gram of polymer for C.I. Basic Violet 3, C.I. Basic Blue 3, and Basic Violet 3, respectively. The differences in adsorption capacities may be due to the effect of dye structure. The negative value of free energy change indicated the spontaneous nature of adsorption.

Keywords: Adsorption; Adsorbent; Cyclodextrin; Basic dyes; Batch study

1. Introduction

Synthetic dyes are an important class of recalcitrant organic compounds and are often found in the environment as a result of their wide industrial use. These industrial pollutants are common contaminants in wastewater. Color is the first contaminant to be recognized in wastewater and the presence of very small amounts of dyes in water is highly visible and undesirable. Neglecting this aesthetic problem, the greatest environmental concern with dyes is their absorption and reflection of sunlight entering the water, which interferes with the growth of bacteria, limiting it to levels insufficient to biologically degrade impurities in the water. It is evident, therefore, that removal of such colored agents from aqueous solutions is of significant environmental and technical importance.

During the past three decades, several physical, chemical and biological decolorization methods have been reported (see Table 1) and attempted for the removal of pollutants from plastics, dyestuffs, textile, pulp and paper effluents; few, however, have been accepted by these industries [1−13]. Amongst the numerous techniques of dye removal, adsorption is the procedure of choice and gives the best result as it can be used to remove different types of coloring materials. This wastewater technique is a well known separation process and is widely used to remove certain classes of chemical pollutants from waters, especially those that are practically unaffected by conventional biological wastewater treatments. Synthetic dyes represent one of the problematic groups. Adsorption has been found to be superior to other techniques for water re-use in terms of initial cost, flexibility and simplicity of design, ease of operation and insensitivity

---

* Tel.: +33 3 81 66 65 64; fax: +33 3 81 66 64 38.
E-mail address: gregorio.crini@univ-fcomte.fr

doi:10.1016/j.dyepig.2007.07.001

Nomenclature

a_L	Langmuir isotherm constant (L mg^{-1})
C_0	initial dye concentration in liquid phase (mg L^{-1})
C_e	liquid phase dye concentration at equilibrium (mg L^{-1})
k	equilibrium rate constant of pseudo-second order sorption (g mg^{-1} min^{-1})
K_F	Freundlich constant (L g^{-1})
K_L	Langmuir isotherm constant (L g^{-1})
q_e	amount of dye adsorbed at equilibrium (mg g^{-1})
q_t	amount of dye adsorbed at time t (mg g^{-1})
q_{max}	maximum adsorption capacity of the adsorbent (mg g^{-1})
m	mass of adsorbent used (g)
n_F	Freundlich isotherm exponent
r^2	non-linear correlation coefficient
R^2	linear correlation coefficient
S	surface area (mg g^{-1})
T	time (min)
t_e	equilibrium time (min)
V	volume of dye solution (L)
x	amount of dye adsorbed (mg)

Greek letter

β	mass transfer coefficient (m s^{-1})

to toxic pollutants. Adsorption also does not result in the formation of harmful substances [9].

Adsorption techniques employing solid adsorbents are effective methods for water decontamination. Most commercial systems currently use activated carbons and organic resins as adsorbents to remove dye in wastewater because of their excellent adsorption abilities [14–16]. A large variety of non-conventional adsorbent materials have been also proposed and studied for their ability to remove dyes [9]. Some of the reported adsorbents include clay materials [17], zeolites [18], siliceous materials [19], agricultural wastes [20,21], industrial by-products [22,23] and biomass [24]. Much attention has recently been focused on biopolymers and natural molecules [25–38] such as chitosan, starch or beta-cyclodextrin.

Table 1
Reviews on existing and emerging technologies for color removal

Technology/reference(s)
Conventional treatment processes
• Physicochemical treatment (sedimentation/flotation, coagulation/flocculation, precipitation, electrokinetic coagulation) [1–3]
• Biodegradation (microbiological decomposition, lagoon, enzymatic treatment, integrated treatment processes) [1–8]
• Adsorption (carbon-based adsorbents, other materials) [1–4,9]
Established recovery processes
• Oxidation (ozonation, electrochemical destruction) [1–3,4,11,12]
• Membrane filtration (ultra-filtration, ion-exchange) [2,13]
Emerging removal processes
• Bioadsorption [9]
• Biomass [2,10]
• Advanced oxidation process (irradiation, photochemical treatment, photocatalysis, sonication) [2,4,12]

Beta-cyclodextrin (CD) is a torus-shaped cyclic oligosaccharide made up of seven α-1,4-linked-D-glucopyranose units with an internal hydrophobic cavity (Fig. 1) [39]. It is well known that this structure gives rise to a remarkable capacity to form inclusion complexes in solution with organic molecules through host–guest interactions. Hence, CD complexation is a procedure of choice for depollution techniques. In the literature, there have been numerous studies on the preparation, characterization, properties and applications of water-insoluble materials containing CD molecules. There are several reported procedures to synthesize these adsorbents and the methods can be generally classified in two ways. First, CD molecules can be polymerized with a coupling agent to form insoluble crosslinked polymers. The second relies on the covalent bonding of CD molecules to a pre-existing insoluble matrix. Two updated reviews of the synthesis of CD-containing adsorbents were given by Crini and Morcellet [40] and Mocanu et al. [41].

Due to the unique structure of the molecule combined with their polyfunctionality, beta-CD molecules have the ability to form crosslinked networks. CD can be crosslinked by a reaction between the hydroxyl groups of the molecules with a coupling agent to form water-insoluble polymeric structures (Fig. 2). One of first and most frequently used crosslinkers is epichlorohydrin (EPI). EPI, containing two reactive functional groups, can react with CD molecules (crosslinking step) and/or itself (polymerization step) [40,41]. The resulting materials are a mixture containing CD units joined by repeating glyceryl linkers. A number of CD rings are interconnected and a three-dimensional network is formed (Fig. 3) [40]. Crosslinked polymers synthesized by condensation between CD and EPI are widely used in chemistry, chromatography, pharmacy, food technology and also for wastewater treatment [39–43]. In particular, it was found that the crosslinked CD polymers exhibited high sorption capacities toward aromatic and phenolic compounds [44,45], naphthalene derivatives [46], dibenzofuran molecules [47,48], metals [49] and dyes [9,36–38,50].

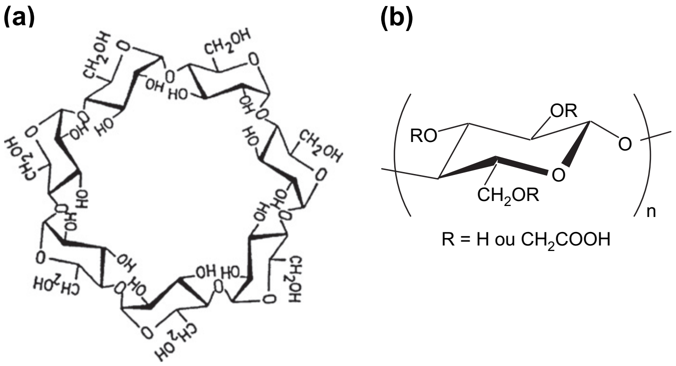

Fig. 1. Chemical structure of (a) beta-cyclodextrin and (b) carboxymethylcellulose.

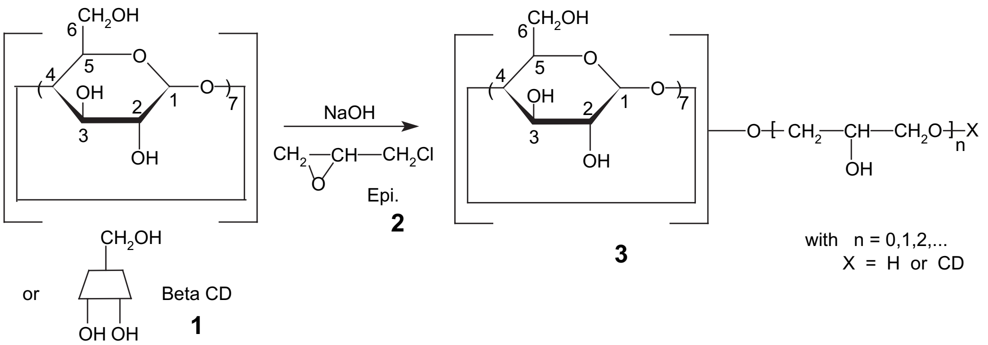

Fig. 2. Synthesis of crosslinked CD-based polymers [40].

In this paper, we propose the use of a cyclodextrin polymer containing carboxylic groups for the sorption of three basic dyes, namely C.I. Basic Blue 3 (BB 3), C.I. Basic Violet 3 (BV 3) and C.I. Basic Violet 10 (BV 10). Studies concerning the effects of contact time and initial dye concentration are presented and discussed. Experimental data were analyzed using pseudo-second order kinetics, mass transfer, and intraparticle diffusion equations. Equilibrium isotherms were analyzed according to Langmuir and Freundlich isotherms. The characteristic parameters for each model have been determined.

2. Materials and methods

2.1. Sorbent

The sorbent has been prepared in one step by reticulation of CD using EPI as crosslinking agent in the presence of carboxymethylcellulose (CMC) (Fig. 1). The synthetic procedure has already been described in detail [51] (see Fig. 4 for the chemical structure of sorbent). The sorbent containing carboxylic and hydroxyl groups (abbreviated CDP) was dried overnight at 100 °C, and then crushed and sieved into different particles sizes. Studies were focused on a size fraction of 150–250 μm. The characteristics of polymer were reported in Table 2. The surface area was 2.4 $m^2 g^{-1}$ (standard BET procedure – N_2 adsorption). This polymeric material has an extremely low surface area compared to that of commercially activated carbons. However, the two most important factors controlling the extent of adsorption properties of cyclodextrin polymers are their hydrophilicity and the crosslink density [40,41,50]. In particular, the polymer possesses a remarkably high swelling capacity in water and, consequently, its network is sufficiently expanded to allow a fast diffusion process for the studied adsorbates. The sample exhibits negative zeta

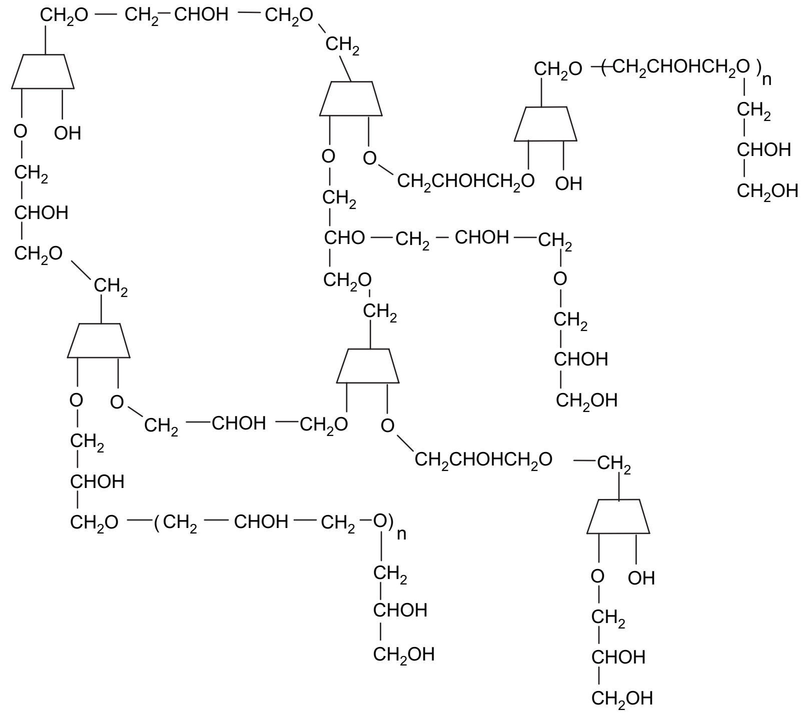

Fig. 3. Structure of an EPI crosslinked CD polymer [40].

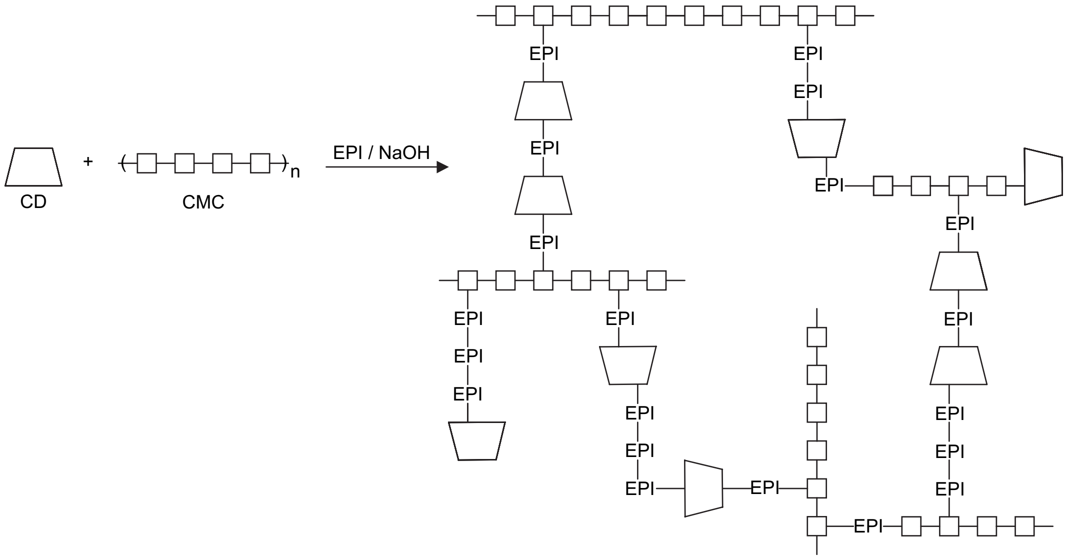

Fig. 4. A possible structure of CDP material containing carboxylic groups.

potential value in the pH range 5–10. The method used for the determination of the amount of CD immobilized onto the polymer (i.e. 420 mg g^{-1}) has been the determination of reducing sugars with tetrazolium blue, as described earlier [45].

2.2. Adsorbate

The adsorption capacity was investigated using BB 3, BV 3 and BV 10 as model guest solutes. These cationic dyes were commercial products and used without purification (see Table 3 and Fig. 5 for the characteristics and structural formulae of each dye, respectively). An accurately weighed quantity of the dye was dissolved in double-distilled water to prepare a stock solution and the solutions for adsorption tests were prepared from the stock solution to the desired concentrations by successive dilutions. The calculated concentrations take into account the dye purity. To calculate the concentration from each experiment, a calibration curve was first prepared for each dye. This curve was used to convert absorbance data into concentrations in kinetic and equilibrium studies.

2.3. Sorption studies and kinetics

Experimental data were determined by the following batch method [52,53]: in each experiment, 100 mg of polymer was mixed with 100 mL of a 0.1 mol L^{-1} NaCl aqueous solution of dye at a known concentration in a tightly closed flask. The presence of inorganic salt significantly promotes the adsorption of dyes on polymers [53]. The pH was adjusted to 8 using either HCl or NaOH. The solution was stirred on a rotating shaker at 25 ± 1 °C. Dye concentration in solution was then measured spectrophotometrically using a UV–vis Uvikon spectrophotometer (UVK-Lab-Serlabo, France). This data was used to calculate the adsorption capacity of the adsorbent. Each experiment was conducted in triplicate under identical conditions and was found reproducible (experimental error within 3%). Blanks containing no dye were conducted at similar conditions as controls. Initial dye concentration in the solution was varied to investigate its effect on the adsorption capacity. Studies were also conducted for various time intervals to determine when adsorption equilibrium was reached and the maximum removal of dye was attained. The amount of dye adsorbed at equilibrium, q_e, was calculated from the mass balance equation given by:

$$q_e = \frac{V(C_0 - C_e)}{m} \tag{1}$$

where C_0 is the initial dye concentration in liquid phase (mg L^{-1}); C_e is the liquid phase dye concentration at equilibrium (mg L^{-1}); V is the volume of dye solution used (L); and m is the mass of sorbent used (g).

Table 2
Characteristics of polymer

Particle size	150–250 μm
BET specific surface area	2.4 m^2 g^{-1}
Swelling capacity	6 mL g^{-1}
C (%)	46.3
Amount of beta-CD[a]	420 mg g^{-1}
Water loss at 125 °C (%)	6.7

[a] From spectrophotometric method.

3. Results and discussion

3.1. Adsorption tests

Adsorption of basic dyes onto CDP was monitored spectrophotometrically by the procedure described in the previous section. Absorbance data obtained using various time intervals were converted into concentration data and then plotted as a function of time in Fig. 6 for each dye. In order to compare adsorption behaviors of dyes, the operating variables (i.e.

Table 3
Characteristics of dyes

Dye	C.I. name	C.I. number	Abbreviation	Molecular weight	Chemical class
Astrazone Blue	Basic Blue 3	51004	BB 3	399.9	Monoxazine
Crystal Violet	Basic Violet 3	42555	BV 3	408.03	Triarylmethane
Rhodamine B	Basic Violet 10	45170	BV 10	479.06	Triarylmethane

initial dye concentration, volume, mass of CDP, temperature and pH) were taken to be the same for the adsorption study of each dye. In particular, the pH for all the experiments was kept at a constant value of 8. Preliminary experiments had shown that maximal capacities were obtained in the pH range 8–11 for C.I. Basic Blue 9 [52] and C.I. Basic Green 4 [53] adsorption onto CDP. The pH of the solution plays an important role in the whole adsorption process, influencing not only the solution dye chemistry, but also the surface charge of the polymer. The polymer contains both hydroxyl and carboxylic groups (at pH 8, these groups are deprotonated) and it was demonstrated that these carboxylic sites were also responsible for dye binding through electrostatic interactions [53]. In alkaline medium, the surface of polymer becomes negatively charged, and therefore the sorption of dye cation by CDP increases at higher pH values and the adsorption takes place more easily.

The dependencies of the concentrations of the dye in solution versus contact time (stirring time) are shown in Fig. 6. The initial dye concentration decreased rapidly with the contact time and this confirmed strong interactions between the dye and the polymer. In other words, the adsorption capacity increased with contact time. Maximum dye was sequestered from the solution within 120 min after the beginning for the three experiments. After that, the concentration of dye in the liquid phase remained almost constant. However, as seen in Fig. 6, at the early stages of adsorption, BV 3 seems to be adsorbed faster than BB 3 but in the later stages the opposite is observed as indicated by the crossover of their corresponding curves in the figure, suggesting a possible effect of the chemical structure of each dye. In this stage of investigations, however, it was not possible to establish a relationship between the dye structure and the sorption rate.

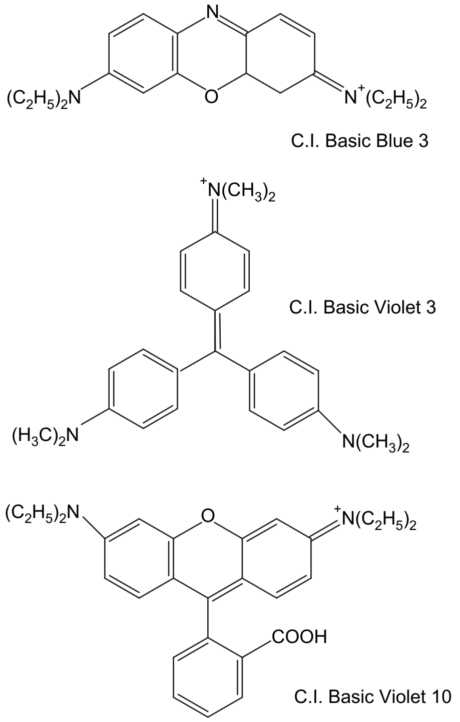

Fig. 5. Chemical structures of basic dyes.

3.2. Dependencies of the adsorbed amounts on time

A simple re-calculation allows to plot the dependencies of the adsorbed amounts (q_t) as functions of contact time (figure not shown). It was shown that adsorption is increased instantly at initial stages due to rapid attachment of dye to the surface of the polymer, and keeps increasing gradually until the equilibrium is reached and remains constant (the remaining concentration becomes asymptotic to the time axis after 90 min of shaking). The amount of dye adsorbed showed no significant difference when the contact times were longer than this; 120 min was found to be sufficient for reaching adsorption equilibrium for the three dyes. These kinetic measurements showed that the process was rapid. The process was also uniform: the time profile of dye uptake was a single, smooth and continuous curve leading to saturation, suggesting the possible monolayer coverage of dye on the surface of the polymer. The order of sorption was: BV 10 > BB 3 > BV 3 and the maximum amounts of basic dye adsorbed were 30.2, 23.9 and 19.8 for BV 10, BB 3 and BV 3, respectively. The difference in the degree of adsorption may be attributed to the chemical

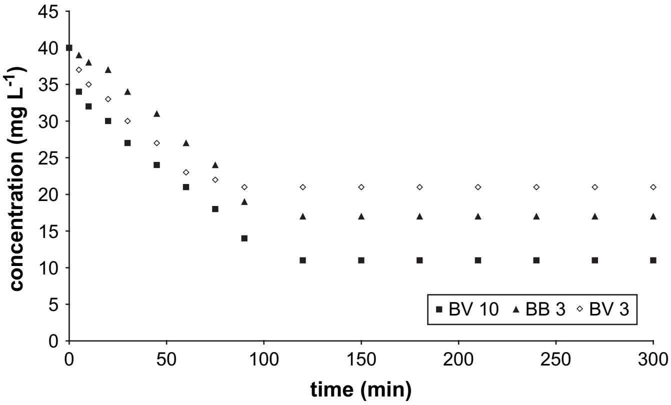

Fig. 6. Decrease of the dye concentration in solution with time for BV 10, BB 3 and BV 3 (conditions: dye concentration = 40 mg L^{-1}; volume = 100 mL; polymer mass = 100 mg; temperature = 25 °C; pH = 8).

structure of each dye. Before discussing this, it is necessary to consider two points: firstly the polymer is an adsorbent that retains the inclusion properties of native cyclodextrin; secondly, the adsorption mechanism is different from those of other materials [50]. The adsorption process consists of several steps: initially the dye molecules migrate from bulk of the solution to the polymer surface (bulk diffusion); the molecules diffuse through the boundary layer to the surface of the adsorbent (film diffusion); then, the molecules diffuse from the surface to the interior of the particle (pore diffusion or intraparticle diffusion); and finally the dye reacts with an active site on the surface of material (chemical reaction).

In previous works [52,53], it was reported that the adsorption mechanism was complex, probably simultaneously dominated by surface adsorption (physical adsorption, hydrogen bonding) and diffusion into the polymer network, chemisorption via the formation of an inclusion complex due to the presence of the CD sites and ion-exchange interactions due to the presence of carboxylic groups. CD molecules have a remarkable capacity to form inclusion complexes (microencapsulation). These complexes are chemical species consisting of two or more associated molecules in which one of the molecules (the host) can admit a guest component into its cavity, resulting in a stable encapsulation without formation of any covalent bonds [39−41]. Several factors play a role in the inclusion complex formation such as hydrophobic effects which induce the apolar group of a molecule to preferentially enter the CD cavity, van der Waals interactions, hydrogen bonding between guest molecule and hydroxyl groups at the rim of the cavity (these contributions increase with polar molecules), solvent effects (release of high-energy water), and also steric effects [39,40]. In particular, the inclusion process is influenced by shape, size and polarity of guest molecules.

The three dyes used in this work differ in their molecular size, chemical class, and functional groups in the molecule (see Fig. 5 and Table 2). So, the differences in the chemical structure between the dyes can explain the curves obtained in Fig. 6. The adsorption is much greater in the case of molecules which present compatible size, steric arrangement and hydrophobicity with the CD. BV 10 displays the best interaction with the polymer: it has a chemical structure which not only may enable a deeper penetration of dye molecules into the polymer network but also favors the formation of an inclusion complex between the dye and the CD sites. BV 3 is a cationic triarylmethane dye and its chemical structure is totally different from the two others. It seems that this structure disfavors sorption (BB 3 forms a less stable inclusion complex): the larger dye molecules do not completely or partly penetrate the polymer, so that the molecules preferentially adsorb near the outer surface of the polymer. Recently, similar observations were reported by Yilmaz Ozmen et al. [36] and Garcia-Zubiri et al. [46] for adsorption of dyes and aromatic compounds on CDP polymers, respectively. Zhang et al. [54], studying the inclusion mechanism between CD and C.I. Basic Blue 9, also reported that the presence of ionic species with electric charge played a role in the interaction between the CD molecules and dyes.

3.3. Adsorption kinetics of basic dyes

The kinetic dependencies were also measured for various initial dye concentrations whereas the other experimental parameters were kept constant (all the experiments here were conducted at pH 8 with the same amount of adsorbent). As example, the dependencies of the q_t values versus the contact time at various concentrations for the blue dye are shown in Fig. 7. Similar trends were obtained for the violet dyes. Again kinetics indicated that the sorption process was uniform with time and can be considered very fast because of the largest amount of dye adsorbed to the polymer within the first 90 min of adsorption. As expected, the overall trend was an increase of the sorption capacity with increasing dye concentrations and this confirmed strong chemical interactions between basic dyes and polymer. However, if the results are expressed in percentage of dye adsorbed, the values decrease when the initial concentration increases.

3.4. Pseudo-second order kinetic model

Four kinetic models, commonly used in the literature, were applied to experimental kinetic data in order to investigate the behavior of dyes on CDP. These models are Lagergren, Ho and McKay, Elovich, and Avrami equations. The validity of each model can be checked from the linear plot. To find the order of kinetics, Lagergren equation was first tested but the straight lines could not be obtained (results not shown). For Lagergren plots, correlation coefficients were below 0.80 and the calculated q_e were not equal to experimental q_e, suggesting the insufficiency of the model to fit kinetic data for the initial concentrations examined. The inapplicability of the Lagergren equation to describe the kinetics of Malachite Green (a basic dye) by adsorption using a CDP polymer was also observed in a previous work [53]. It was reported that, after a short period, the experimental data deviated considerably from linearity (the model did not fit the data well for the whole range of contact time and underestimated the q_e values). Elovich and Avrami models were also adopted to examine the mechanism

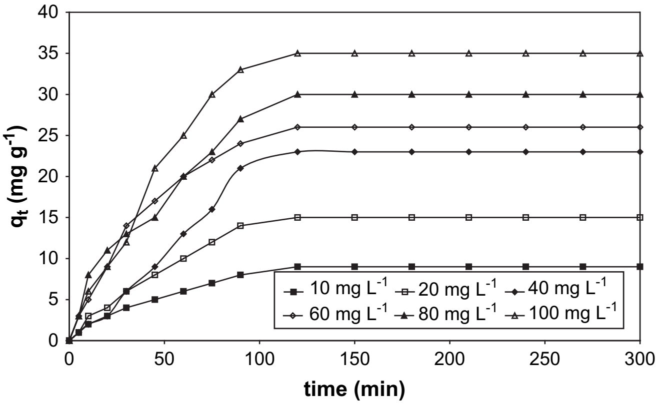

Fig. 7. Kinetics of adsorption capacity of C.I. Basic Blue 3 (BB 3) by CDP material for various initial dye concentrations (conditions: volume = 100 mL; polymer mass = 100 mg; temperature = 25 °C; pH = 8).

of the adsorption process, but the straight lines could not be obtained. Then, kinetics of basic dyes on CDP were analyzed using the Ho and McKay model.

The pseudo-second order model proposed by Ho and McKay can be represented in the following linear form [55,56]:

$$\frac{t}{q_t}=\frac{1}{k_2 q_e^2}+\frac{1}{q_e}t \tag{2}$$

where q_t and q_e are the amount adsorbed at time t and at equilibrium (mg g^{-1}), respectively; k_2 is the pseudo-second order rate constant for the adsorption process (g mg^{-1} min^{-1}).

The rate parameters k_2 and q_e can be directly obtained from the intercept and slope of the plot of t/q_t versus t. If the pseudo-second order kinetics is applicable, the plot gives a linear relationship which allows computation of k_2 and q_e without having known any parameter beforehand. These parameters obtained by linear regression are reported in Table 4. The results showed that the adsorption system followed the Ho and McKay equations for the entire adsorption period, with regression coefficients higher than 0.995 for the concentration range used in this study. The calculated q_e values from the model were also in good agreement with the experimental values. Kinetics of basic dyes' adsorption on CDP followed the pseudo-second order model, suggesting that the rate-limiting step may be chemisorption [55,56]. This confirmed that adsorption of dye takes place probably via surface exchange reactions until the surface functional sites are fully occupied; thereafter dye molecules diffuse into the polymer network for further interactions (such as inclusion complex, hydrogen bonding, hydrophobic interactions). The obtained k_2 values were plotted against the initial dye concentration (figure not shown). It was observed that there was no linear relationship between the rate constants and concentration [53]. No distinct relationship can be also established between the k_2 values and the structure of the dye.

Table 4
Pseudo-second order kinetic constants for basic dyes sorption onto CDP material

Dye	C_0 (mg g^{-1})	$q_{e\ exp}$ (mg g^{-1})	k_2 (g mg^{-1} min^{-1})	$q_{e\ cal}$ (mg g^{-1})	R^2
BV 10	10	10.1	3.01×10^{-3}	10.7	0.9951
	20	19.5	8.55×10^{-4}	20.1	0.9915
	40	30.2	8.40×10^{-4}	31.5	0.9892
	60	34.3	7.19×10^{-4}	36.1	0.9965
	80	39.5	6.53×10^{-4}	40.8	0.9855
	100	43.2	5.34×10^{-4}	46.1	0.9925
BB 3	10	9.3	2.21×10^{-3}	10.6	0.9901
	20	17.2	9.46×10^{-4}	17.8	0.9916
	40	23.9	1.79×10^{-4}	27.3	0.9716
	60	27.2	8.45×10^{-4}	30.1	0.9902
	80	31.1	6.58×10^{-4}	32.5	0.9868
	100	37.2	4.32×10^{-4}	40.4	0.9810
BV 3	10	7.2	5.71×10^{-3}	7.8	0.9951
	20	11.3	4.73×10^{-3}	11.7	0.9982
	40	19.8	3.90×10^{-3}	20.1	0.9913
	60	21.5	2.96×10^{-3}	22.3	0.9988
	80	25.3	3.16×10^{-3}	26.3	0.9986
	100	30.1	1.16×10^{-3}	32.3	0.9946

The kinetics of adsorption of many dye species onto various adsorbents was also found to be of second order in the literature [22,24,25,32,57,58]. The k_2 values obtained in this study were comparable to those of the other available materials. The pseudo-second order model is commonly used to describe kinetics of dye adsorption on solid adsorbents, although as pointed out by Ho and McKay [56], the application of a single kinetic model to the adsorption on materials may be questionable because of the heterogeneity of the adsorbent surfaces and diversity of adsorption phenomena (transport, diffusion, reactions).

3.5. Mass transfer coefficient

Mass transfer coefficients (β) of basic dyes at the polymer–solution interface were determined by using the following equation [59]:

$$\ln\left(\frac{C_t}{C_0}-\frac{1}{1+mK_L}\right)=\ln\left(\frac{mK_L}{1+mK_L}\right)-\left(\frac{1+mK_L}{mK_L}\right)\beta St \tag{3}$$

where K_L is the Langmuir constant, m the mass of adsorbent, and S the surface area of polymer.

In plotting the curves, K_L values for the adsorption of basic dyes onto CDP were taken from the results indicated below. Linear graphical relations between $\ln[(C_t/C_0) - 1/(1 + mK_L)]$ versus t were not obtained, indicating the inapplicability of this model.

3.6. Intraparticle diffusion model

The dye sorption is governed usually by either the liquid phase mass transport rate or the intraparticle mass transport rate. Hence diffusive mass transfer is incorporated into the adsorption process. In diffusion studies, the rate can be expressed in terms of the square root time. The mathematical dependence of q_t versus $t^{1/2}$ (known as the Weber–Morris plot) is obtained if the process is considered to be influenced by diffusion in the particles and convective diffusion in the solution [59,60].

According to the intraparticle diffusion model proposed by Weber–Morris [60], the root time dependence may be expressed by the following equation:

$$q_t = k_i t^{1/2} \tag{4}$$

where q_t is the amount of dye on the surface of the polymer at time t (mg g^{-1}), t the time (min), and k_i the intraparticle diffusion rate constant (mg g^{-1} min$^{-0.5}$).

Fig. 8 shows the amount of dye adsorbed versus $t^{1/2}$ for intraparticle transport of BV 10 by CDP adsorbent at different initial dye concentrations. Similar trends were obtained for BB 3 and BV 3. The results showed that the plots presented a multilinearity which indicated that two or more steps occurred in the process. The R^2 values for this diffusion model were between 0.9602 and 0.9969, suggesting that the adsorption of BB 9 onto CDP material can be followed by an

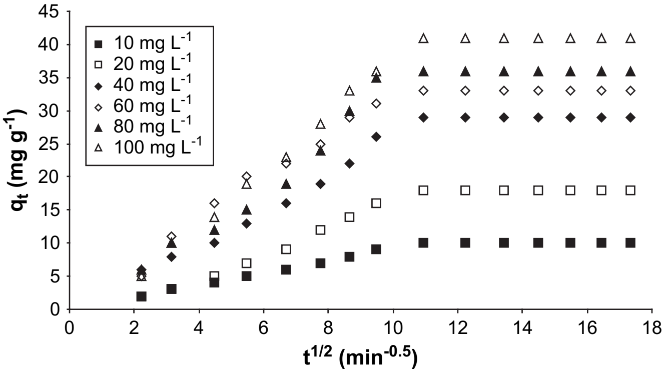

Fig. 8. Dependencies of q_t versus $t^{0.5}$ (intraparticle diffusion model) for BV 10 on CDP (conditions: volume = 100 mL; polymer mass = 100 mg; temperature = 25 °C; pH = 8).

intraparticle diffusion model. It can be also observed that the plots did not pass through the origin; this was indicative of some degree of boundary layer control and this further showed that the intraparticle diffusion was not the only rate-limiting step, but other processes might control the rate of adsorption. The slope of the linear portion characterizes the rate parameter k_i corresponding to the intraparticle diffusion (the values for each initial concentration are given in Table 5). It was found that the rate constant increased with increasing dye concentration. Table 6 presents the results of fitting experimental data with pseudo-second order and intraparticle models using linear (R^2) and non-linear (r^2) coefficients of determination, and also a normalized percent deviation test (P). P is defined by the following equation:

$$P = \left(\frac{100}{N}\right) \sum \left(\frac{|q_{t,\mathrm{exp}} - q_{t,\mathrm{cal}}|}{q_{t,\mathrm{exp}}} \right) \tag{5}$$

where $q_{t,\mathrm{exp}}$ is the experimental data at any t, $q_{t,\mathrm{cal}}$ is the corresponding predicted q_t according to the model under study with best fitted parameters, and N the number of data points; the lower P value, the better is the fit.

Table 5
Intraparticle diffusion rate constants for the adsorption of basic dyes onto CDP

Dye	C_0 (mg g^{-1})	k_i (mg g^{-1} min$^{-1/2}$)	R^2
BV 10	10	0.937	0.9969
	20	1.926	0.9862
	40	2.669	0.9805
	60	3.372	0.9792
	80	3.802	0.9602
	100	4.222	0.9964
BB 3	10	0.937	0.9969
	20	1.737	0.9875
	40	2.691	0.9402
	60	3.010	0.9910
	80	3.025	0.9771
	100	4.325	0.979
BV 3	10	0.598	0.9919
	20	0.865	0.9048
	40	2.356	0.9867
	60	1.924	0.9584
	80	2.865	0.9965
	100	2.537	0.9979

Table 6
Comparison of linear (R^2) and non-linear (r^2) regression coefficients of determination, and normalized percent deviation (P) for pseudo-second order and intraparticle diffusion models

Dye	C_0 (mg g^{-1})	Pseudo-second order			Intraparticle diffusion		
		R^2	r^2	P	R^2	r^2	P
BV 10	10	0.9951	0.9853	3.12	0.9969	0.7989	9.20
	20	0.9915	0.9807	3.09	0.9862	0.7954	9.63
	40	0.9892	0.9821	3.32	0.9805	0.7988	10.24
	60	0.9965	0.9881	3.57	0.9792	0.7996	9.57
	80	0.9855	0.9789	3.62	0.9602	0.8147	10.39
	100	0.9925	0.9792	3.41	0.9964	0.8176	9.99
BB 3	10	0.9901	0.9824	4.34	0.9969	0.8021	17.20
	20	0.9916	0.9833	4.21	0.9875	0.8004	17.65
	40	0.9716	0.9657	4.68	0.9402	0.8112	18.45
	60	0.9902	0.9796	4.98	0.9910	0.8240	18.87
	80	0.9868	0.9777	5.02	0.9771	0.8337	17.55
	100	0.9810	0.9778	5.32	0.979	0.8277	18.40
BV 3	10	0.9951	0.9857	4.76	0.9919	0.6981	23.11
	20	0.9982	0.9878	4.21	0.9048	0.6989	24.37
	40	0.9913	0.9801	4.99	0.9867	0.7021	24.66
	60	0.9988	0.9788	5.02	0.9584	0.7008	25.39
	80	0.9986	0.9654	5.32	0.9965	0.7108	25.51
	100	0.9946	0.9698	5.28	0.9979	0.7155	26.21

From the Table 5, the comparison of error analysis showed that the order of deviation was Weber–Morris model > Ho–McKay model, which indicated that the pseudo-second order equation was the best one in describing the adsorption kinetics of basic dyes on CDP material. This model was better adjusted specially for BV 10.

3.7. Adsorption isotherms

Adsorption isotherms describe how pollutants interact with sorbent materials and so, are critical in optimizing the use of adsorbents. In order to optimize the design of an adsorption system to remove dye from solutions, it is important to establish the most appropriate correlation for the equilibrium curve. There are several isotherm equations available for analyzing experimental sorption equilibrium data [61]. Four isotherm equations have been tested in the present study, namely generalized, Temkin, Toth, and Redlich–Peterson. Applicability of these equations was compared by judging the correlation coefficients and P values. However, the fits of the experimental data were poor (the straight lines could not be obtained). Then, experimental data were fitted to well-known and widely applied isotherm models of Langmuir [62,63] and Freundlich [64]. The linear equations are given below:

$$\text{Langmuir}: \frac{C_\mathrm{e}}{q_\mathrm{e}} = \frac{1}{K_\mathrm{L}} + \frac{a_\mathrm{L}}{K_\mathrm{L}} C_\mathrm{e} \tag{6}$$

$$\text{Freundlich}: \ln q_\mathrm{e} = \ln K_\mathrm{F} + \frac{1}{n_\mathrm{F}} \ln C_\mathrm{e} \tag{7}$$

where C_e (mg L^{-1}) and q_e (mg g^{-1}) are the liquid phase concentration and solid phase concentration of adsorbate at equilibrium, respectively; K_L (L^{-1} mg) and a_L (L^{-1} mg) are the Langmuir isotherm constants; K_F is the Freundlich constant (L^{-1} mg), and $1/n_F$ is the heterogeneity factor.

By plotting C_e/q_e against C_e (Fig. 9), it was possible to obtain the value of K_L from the intercept which was $1/K_L$ and the value of a_L from the slope which was a_L/K_L. The maximum adsorption capacity of the adsorbent (q_{max}) is numerically equal to K_L/a_L. The plot of ln q_e versus C_e was employed to generate the intercept value of K_F and the slope $1/n_F$ (Fig. 10). $1/n_F$ is a measure of the deviation from linearity of the adsorption. The value ranges between 0 and 1, and indicates the degree of non-linearity between solution concentration and adsorption as follows: if the value of $1/n_F$ is equal to unity, the adsorption is linear; if the value is below unity, this implies that adsorption process is chemical; if value is above unity, adsorption is a favorable physical process. The more heterogeneous the surface, the closer $1/n_F$ value is to 0 [65]. The Langmuir and Freundlich isotherm parameters for the adsorption of basic dyes onto CDP are listed in Table 7. The adsorption behavior of dyes was analyzed using both linear and non-linear regression.

The linearized forms of Langmuir and Freundlich isotherms are found to be linear over the whole concentration range studied. Apparently, the plots in Figs. 9 and 10, and the R^2 values (>0.98) showed that the two equations provided a reasonable description of the experimental data. However, examination of the results by non-linear regression suggested that the Freundlich model (with $r^2 > 0.99$) yielded a much better fit than the Langmuir model (Table 7). In addition, the P values for the linear form of the Langmuir isotherm were very large (especially in the case of BV 3), suggesting that the isotherm constants of this model did not describe well the equilibrium data. The values of $n_F > 1$ reflected the favorable adsorption. The Freundlich isotherm, the earliest known relationship describing the adsorption process, is an empirical equation employed to describe heterogeneous systems. Its application suggests that adsorption energy exponentially decreases on completion of the sorptional centres of an adsorbent. The Langmuir equation is applicable to homogeneous adsorption, where the adsorption of each molecule onto the surface has equal adsorption activation energy. On the basis of the Langmuir analysis, the maximum adsorption capacities were determined to be 53.2, 42.4 and 35.8 mg of dye per gram of polymer for BV 10, BB 3 and BV 3, respectively. These values demonstrated that CDP material exhibited interesting sorption properties. Compared with some recent data in the literature [9], the results also revealed the potential of CDP to be an effective adsorbent for removing basic dyes.

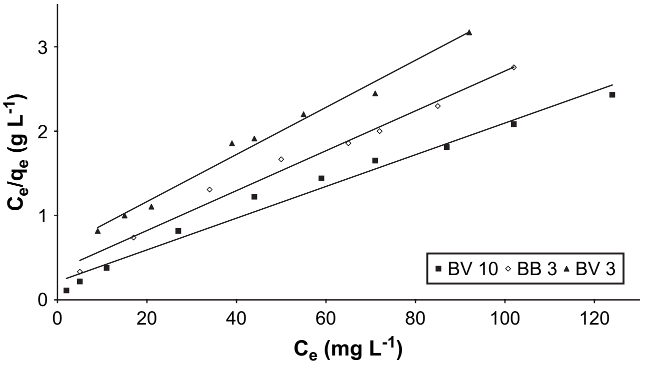

Fig. 9. Langmuir plots for the adsorption of basic dyes onto CDP material.

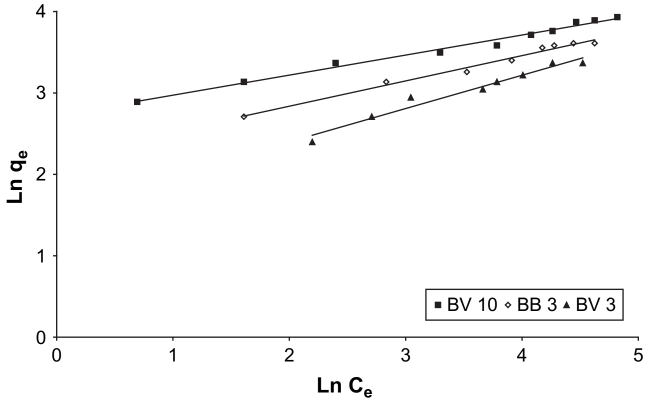

Fig. 10. Freundlich plots for the adsorption of basic dyes onto CDP material.

The essential features of the Langmuir isotherm can be expressed in terms of a dimensionless constant called separation factor (R_L, also called equilibrium parameter) which is defined by the following equation [66]:

$$R_L = \frac{1}{1 + a_L C_0} \tag{8}$$

where C_0 is the initial concentration (mg l^{-1}) and a_L is the Langmuir constant related to the energy of adsorption (L mg^{-1}).

The value of R_L indicates the shape of the isotherms to be either unfavorable ($R_L > 1$), linear ($R_L = 1$), favorable ($0 < R_L < 1$) or irreversible ($R_L = 0$) [67]. It was observed that the value of R_L

Table 7
Summary of the Langmuir and Freundlich isotherm constants, and comparison of linear (R^2) and non-linear (r^2) regression coefficients of determination and the normalized percent deviation (P)

Dye	Model	Parameters	R^2	r^2	P
BV 10	Langmuir	$q_{max} = 53.2$ (mg g^{-1}), $K_L = 4.61$ (L g^{-1}), $a_L = 0.087$ (L mg^{-1}), $R_L = 0.534–0.103$	0.9809	0.9724	6.98
	Freundlich	$K_F = 15.27$ (L g^{-1}), $n_F = 4.06$	0.9894	0.9967	1.85
BB 3	Langmuir	$q_{max} = 42.4$ (mg g^{-1}), $K_L = 2.87$ (L g^{-1}), $a_L = 0.068$ (L mg^{-1}), $R_L = 0.595–0.128$	0.9849	0.9787	9.67
	Freundlich	$K_F = 9.17$ (L g^{-1}), $n_F = 3.22$	0.9858	0.9913	3.24
BV 3	Langmuir	$q_{max} = 35.8$ (mg g^{-1}), $K_L = 1.65$ (L g^{-1}), $a_L = 0.046$ (L mg^{-1}), $R_L = 0.684–0.178$	0.9857	0.9708	10.79
	Freundlich	$K_F = 4.86$ (L g^{-1}), $n_F = 2.45$	0.9742	0.9911	4.11

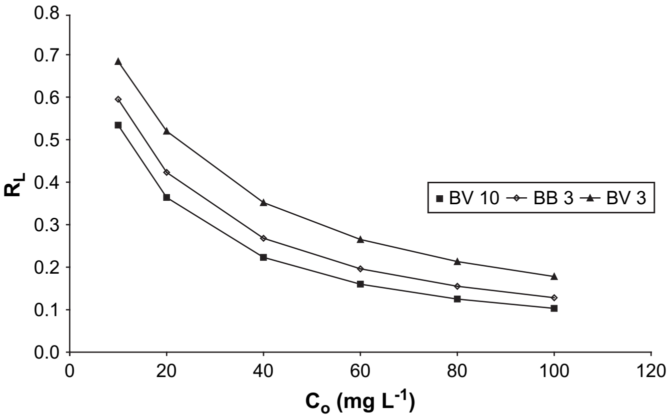

Fig. 11. Separation factor for basic dyes onto CDP material at 25 °C.

in the range of 0–1 (Table 7) confirmed the favorable uptake of the dye process. The calculated R_L values at different initial dye concentration are reported in Fig. 11. Also higher R_L values at lower dye concentrations showed that adsorption was more favorable at lower concentration.

The free energy change (ΔG) for adsorption at 25 °C was calculated using the following equation:

$$\Delta G = -RT \ln K_L \tag{9}$$

where T is the temperature, R the gas constant, and K_L the Langmuir constant.

The calculated ΔG values were found to be −962.3, −391.2 and −519.8 J mol^{-1} for BV 10, BB 3 and BV 3, respectively. The negative value of free energy change indicated the spontaneous nature of sorption and confirmed affinity of sorbent for the dyes.

4. Conclusions

Equilibrium and kinetic studies were made for the adsorption of basic dyes from aqueous solutions onto a cyclodextrin polymer. This adsorbent exhibited high sorption capacities: the monolayer adsorption capacities were 53.2, 42.4 and 35.8 mg of dye per gram of polymer for BV 10, BB 3 and BV 3, respectively. The straight lines in plots of t/q_t versus t showed good agreement of experimental data with the second-order kinetic model for different initial sorbent concentration, suggesting that the adsorption process might be chemisorption. The equilibrium data have been analyzed using Langmuir and Freundlich models. The results showed that experimental data were correlated reasonably well by the Freundlich adsorption isotherm. The negative value of free energy change indicated the spontaneous nature of sorption. The differences in adsorption capacities may be due to the effect of dye structure. To confirm this, more experiments will be carried out using other similar basic dyes.

Acknowledgements

The author thanks Capucine Robert, Nadia Morin-Crini and Brigitte Jolibois (University of Franche-Comté) for assistance during this work, and OSEO/ANVAR and ANR for financial supports.

References

[1] Pokhrel D, Viraraghavan T. Treatment of pulp and paper mill wastewater – a review. The Science of the Total Environment 2004;333:37–58.
[2] Robinson T, McMullan G, Marchant R, Nigam P. Remediation of dye in textile effluent: a critical review on current treatment technologies with a proposed alternative. Bioresource Technology 2001;77:247–55.
[3] Anjaneyulu Y, Sreedhara Chary N, Samuel Suman Raj D. Decolourization of industrial effluents-available methods and emerging technologies – a review. Reviews in Environmental Science and Bio/Technology 2005; 4:245–73.
[4] Forgacs E, Cserhati T, Oros G. Removal of synthetic dyes from wastewaters: a review. Environment International 2004;30:953–71.
[5] Thompson G, Swain J, Kay M, Forster CF. The treatment of pulp and paper mill effluent: a review. Bioresource Technology 2001;77:275–86.
[6] Singh Rai H, Bhattacharyya MS, Singh J, Bansal TK, Vats P, Banerjee UC. Removal of dyes from the effluent of textile and dyestuff manufacturing industry: a review of emerging techniques with reference to biological treatment. Critical Reviews in Environmental Science and Technology 2005;35:219–38.
[7] Pearce CI, Lloyd JR, Guthrie JT. The removal of colour from textile wastewater using whole bacterial cells: a review. Dyes and Pigments 2003;58:179–96.
[8] Fu Y, Viraraghavan T. Fungal decolorization of dye wastewaters – a review. Bioresource Technology 2001;79:251–62.
[9] Crini G. Non-conventional low-cost adsorbents for dye removal: a review. Bioresource Technology 2006;97:1061–85.
[10] Aksu Z. Application of biosorption for the removal of organic pollutants: a review. Process Biochemistry 2005;40:997–1026.
[11] Vajnhandl S, Majcen le Marechal A. Ultrasound in textile dyeing and the decolouration/mineralization of textile dyes. Dyes and Pigments 2005;65:89–101.
[12] Guivarch E, Oturan MA. Le problème de la contamination des eaux par les colorants synthétiques: comment les détruire? Application du procédé électro-Fento. L'Actualité Chimique 2004;277/278:65–9.
[13] Hilal N, Al-Zoubi H, Darwish NA, Mohammad AW, Abu Arabi M. A comprehensive review of nanofiltration membranes: treatment, pretreatment, modeling, and atomic force microscopy. Desalination 2004;170:281–308.
[14] Orfao JJM, Silva AIM, Pereira JCV, Barata SA, Fonseca IM, Faria PCC, et al. Adsorption of a reactive dye on chemically modified activated carbons – influence of pH. Journal of Colloid and Interface Science 2006;296:480–9.
[15] Attia AA, Rashwan WE, Khedr SA. Capacity of activated carbon in the removal of acid dyes subsequent to its thermal treatment. Dyes and Pigments 2006;69:128–36.
[16] Derbyshire F, Jagtoyen M, Andrews R, Rao A, Martin-Gullon I, Grulke E. In: Radovic LR, editor. Carbon materials in environmental applications. Chemistry and physics of carbon, vol. 27. New York: Marcel Dekker; 2001. p. 1–66.
[17] Alkan M, Celikçapa S, Demirbas Ö, Dogan M. Removal of reactive blue 221 and acid blue 62 anionic dyes from aqueous solutions by sepiolite. Dyes and Pigments 2005;65:251–9.
[18] Armagan B, Turan M, Celik MS. Equilibrium studies on the adsorption of reactive azo dyes into zeolite. Desalination 2004;170:33–9.
[19] Walker GM, Hansen L, Hanna JA, Allen SJ. Kinetics of a reactive dye adsorption onto dolomitic sorbents. Water Research 2003;37:2081–9.

[20] Aksu Z, Isoglu IA. Use of dried sugar beet pulp for binary biosorption of Gemazol Turquoise Blue-G reactive dye and copper(II) ions: equilibrium modeling. Chemical Engineering Journal 2007;127:177–88.

[21] Han R, Zou W, Yu W, Cheng S, Wang, Shi J. Biosorption of methylene blue from aqueous solution by fallen phoenix tree's leaves. Journal of Hazardous Materials 2007;141:156–62.

[22] Noroozi B, Sorial GA, Bahrami H, Arami M. Equilibrium and kinetic adsorption study of a cationic dye by a natural adsorbent – silkworm pupa. Journal of Hazardous Materials 2007;B139:167–74.

[23] Golder AK, Samanta AN, Ray S. Anionic reactive dye removal from aqueous solution using a new adsorbent – sludged generated in removal of heavy metal by electrocoagulation. Chemical Engineering Journal 2006;122:107–15.

[24] Vijayaraghavan K, Yun YS. Utilization of fermentation waste (*Corynebacterium glutamicum*) for biosorption of reactive black 5 from aqueous solution. Journal of Hazardous Materials 2007;141:45–52.

[25] Stephen Inbaraj B, Chien JT, Ho GH, Yang J, Chen BH. Equilibrium and kinetic studies on sorption of basic dyes by a natural biopolymer poly(γ-glutamic acid). Biochemical Engineering Journal 2006;31:204–15.

[26] Paulino AT, Guilherme MR, Reis AV, Campese GM, Muniz EC, Nozaki J. Removal of methylene blue dye from an aqueous media using superabsorbent hydrogel supported on modified polysaccharide. Journal of Colloid and Interface Science 2006;301:55–62.

[27] Davila-Jiménez MM, Elizalde-Gonzalez MP, Pelaez-Cid AA. Adsorption interaction between natural adsorbents and textile dyes in aqueous solution. Colloids and Surfaces A Physicochemistry Engineering Aspects 2005;254:107–14.

[28] Blackburn RS. Natural polysaccharides and their interactions with dye molecules: applications in effluent treatment. Environmental Science Technology 2004;38:4905–9.

[29] No HK, Meyers SP. Application of chitosan for treatment of wastewaters. Reviews of Environmental Contamination and Toxicology 2000;163: 1–28.

[30] Klimaviciute R, Riauka A, Zemaitaitis A. The binding of anionic dyes by cross-linked cationic starches. Journal of Polymer Research 2007;14: 67–73.

[31] Abdel-Aal SE, Gad YH, Dessouki AM. Use of rice straw and radiation-modified maize starch/aceylonitrile in the treatment of wastewater. Journal of Hazardous Materials 2006;B129:204–15.

[32] Xu S, Wang J, Wu R, Wang J, Li H. Adsorption behaviors of acid and basic dyes on crosslinked amphoteric starch. Chemical Engineering Journal 2006;117:161–7.

[33] Delval F, Crini G, Morin N, Vebrel J, Bertini S, Torri G. The sorption of several types of dye on crosslinked polysaccharides derivatives. Dyes and Pigments 2002;53:79–92.

[34] Wong YC, Szeto YS, Cheung WH, McKay G. Adsorption of acid dyes on chitosan-equilibrium isotherm analyses. Process Biochemistry 2004; 39:693–702.

[35] Cestari AR, Vieira AFS, dos Santos AGP, Mota JA, de Almeida VP. Adsorption of anionic dyes on chitosan beads. 1. The influence of the chemical structures of dyes and temperature on the adsorption kinetics. Journal of Colloid and Interface Science 2004;280:380–6.

[36] Yilmaz Ozmen E, Sirit A, Yilmaz M. A calix[4]arene oligomer and two beta-cyclodextrin polymers: synthesis and sorption studies of azo dyes. Journal of Macromolecular Science Part A Pure and Applied Chemistry 2007;44:167–73.

[37] Gaffar MA, El-Rafie SM, El-Tahlawy KF. Preparation and utilization of ionic exchange resin via graft copolymerization of beta-CD itaconate with chitosan. Carbohydrate Polymers 2004;56:387–96.

[38] Martel B, Devassine M, Crini G, Weltrowski M, Bourdonneau M, Morcellet M. Preparation and sorption properties of a beta-cyclodextrin-linked chitosan derivative. Journal of Polymer Science Part A Polymer Chemistry 2001;394:169–73.

[39] Szejtli J. Introduction and general overview of cyclodextrin. Chemical Review 1998;98:1743–53.

[40] Crini G, Morcellet M. Synthesis and applications of adsorbents containing cyclodextrins. Journal of Separation Science 2002;25: 789–813.

[41] Mocanu G, Vizitiu D, Carpov A. Cyclodextrin polymers. Journal of Bioactive and Compatible Polymers 2001;16:315–42.

[42] Szejtli J. Cyclodextrins and their inclusion complexes. Dordrecht: Kluwer Academic Publishers; 1988.

[43] Duchêne D, editor. Cyclodextrins and their industrial uses. Paris: Editions de Santé, France; 1987.

[44] Flores J, Jiménez V, Belmar J, Mansilla HD, Alderete JB. Inclusion complexation of phenol derivatives with a beta-cyclodextrin based polymer. Journal of Inclusion Phenomena and Macrocyclic Chemistry 2005; 53:63–8.

[45] Crini G, Bertini S, Torri G, Naggi A, Sforzini D, Vecchi C, et al. Sorption of aromatic compounds in water using insoluble cyclodextrin polymers. Journal of Applied Polymer Science 1998;68:1973–8.

[46] Garcia-Zubiri I, Gonzalez-Gaitano G, Isasi JR. Thermal stability of solid dispersions of naphthalene derivatives with beta-cyclodextrin and beta-cyclodextrin polymers. Thermochimica Acta 2006;444:57–64.

[47] Romo A, Penas FJ, Isasi JR. Sorption of dibenzofuran derivatives from aqueous solutions by beta-cyclodextrin polymers: an isosteric heat approach. Journal of Colloid and Interface Science 2004;279:55–60.

[48] Sainz-Rozas PR, Isasi JR, Gonzalez-Gaitano G. Binding of dibenzofuran and its derivatives to water-soluble beta-cyclodextrin polymers. Journal of Photochemistry and Photobiology A Chemistry 2005;173:248–57.

[49] Girek T, Kozlowski CA, Koziol JJ, Walkowiak W, Korus I. Polymerisation of beta-cyclodextrin with succinic anhydride. Synthesis, characterization, and ion flotation of transition metals. Carbohydrate Polymers 2005;59:211–5.

[50] Crini G. Recent developments in polysaccharide-based materials used as adsorbents in wastewater treatment. Progress in Polymer Science 2005;30:38–70.

[51] Crini G, Morin N, Rouland JC, Janus L, Morcellet M, Bertini S. Adsorption de béta-naphtol sur des gels de cyclodextrines-carboxyméthylcelluloses réticulés. European Polymer Journal 2002;38:1095–103.

[52] Crini G, Peindy HN. Adsorption of C.I. Basic Blue 9 on cyclodextrin-based material containing carboxylic groups. Dyes and Pigments 2006;70:204–11.

[53] Crini G, Peindy HN, Gimbert F, Robert C. Removal of C.I. Basic Green 4 (Malachite Green) from aqueous solutions by adsorption using cyclodextrin-based adsorbent: kinetic and equilibrium studies. Separation and Purification Technology 2007;53:97–110.

[54] Zhang G, Shuang S, Dong C, Pan J. Study on the interaction of methylene blue with cyclodextrin derivatives by absorption and fluorescence spectroscopy. Spectrochimica Acta Part A 2003;59:2935–41.

[55] Ho YS, Mc Kay G. A comparison of chemisorption kinetic models applied to pollutant removal on various sorbents. Process Safety and Environmental Protection 1998;76:332–40.

[56] Ho YS, Mc Kay G. Kinetic of sorption of basic dyes from aqueous solution by sphagnum moss peat. Canadian Journal of Chemical Engineering 1998;76:822–7.

[57] Gücek A, Sener S, Bilgen S, Mazmanci MA. Adsorption and kinetic studies of cationic and anionic dyes on pyrophyllite from aqueous solution. Journal of Colloid and Interface Science 2005;286:53–60.

[58] Arami M, Limaee NY, Mahmoodi NM, Tabrizi NS. Removal of dyes from colored textile wastewater by orange peel adsorbent: equilibrium and kinetic studies. Journal of Colloid and Interface Science 2005; 288:371–6.

[59] (a) Furusawa T, Smith JM. Fluid-particle and intraparticle mass transport rates in slurries. Industrial and Engineering Chemistry Fundamentals 1973;12:197–203;
(b) Furusawa T, Smith JM. Intraparticle mass transport in slurries by dynamic adsorption studies. American Institute of Chemical Engineers Journal 1974;20:88–93.

[60] Weber WJ, Morris J. Kinetics of adsorption on carbon from solution. Journal of the Sanitary Engineering Division, Proceedings of the American Society of Civil Engineers 1963;31–59. SA2.

[61] Tien C. Adsorption calculations and modeling. Newton, Boston, USA: Butterworth-Heinemann; 1994.

[62] Langmuir I. The constitution and fundamental properties of solids and liquids. Journal of American Chemical Society 1916;38:2221–95.

[63] Langmuir I. The adsorption of gases on plane surfaces of glass, mica and platinum. Journal of American Chemical Society 1918;40:1361–403.
[64] Freundlich HMF. Über die adsorption in lösungen. Zeitschrift für Physikalische Chemie 1906;57:385–471.
[65] Al-Duri B. Adsorption modeling and mass transfer. In: McKay G, editor. Use of adsorbents for the removal of pollutants from wastewaters. Florida: CRC Press Inc.; 1995. p. 133–73.
[66] Hall KR, Eagleton LC, Acrivos A, Vermeulen T. Pore- and solid-diffusion kinetics in fixed-bed adsorption under constant-pattern conditions. Industrial and Engineering Chemistry Fundamentals 1966; 5:212–23.
[67] Weber TW, Chakravorti RK. Pore and solid diffusion models for fixed bed adsorbers. American Institute of Chemical Engineers Journal 1974;20:228–38.